Author/s:
Masoomi-Godarzi, S;Liu, M;Tachibana, Y;Goerigk, L;Ghiggino, KP;Smith, TA;Jones, DJ

Title:
Solution-Processable, Solid State Donor–Acceptor Materials for Singlet Fission

Date:
2018-10-25

Citation:
Masoomi-Godarzi, S., Liu, M., Tachibana, Y., Goerigk, L., Ghiggino, K. P., Smith, T. A. & Jones, D. J. (2018). Solution-Processable, Solid State Donor–Acceptor Materials for Singlet Fission. Advanced Energy Materials, 8 (30), https://doi.org/10.1002/aenm.201801720.

Persistent Link:
https://hdl.handle.net/11343/284496

DOI: 10.1002/ ((please add manuscript number))

Article type: Full Paper

Solution-processable, solid state donor-acceptor materials for singlet fission

Saghar Masoomi-Godarzi[ab], Maning Liu[c], Yasuhiro Tachibana[c], Lars Goerigk[b], Kenneth P. Ghiggino[b], Trevor A. Smith[b] and David J. Jones[ab]*

[a] Bio21 Institute and [b] School of Chemistry, University of Melbourne, Parkville, Victoria 3010, Australia.

[c] School of Engineering, RMIT University, Bundoora, Victoria 3083, Australia.

[*] Email: djjones@unimelb.edu.au

Keywords: Singlet fission, photophysics, organic photovoltaics, intramolecular singlet fission

Abstract

The exploitation of singlet fission (SF) materials in optoelectronic devices is restricted by the limited number of SF materials available and developing new organic materials that undergo singlet fission is a significant challenge. Using new strategy based on conjugating strong donor and acceptor building blocks, we have designed and synthesized the small molecule ($BDT(DPP)_2$) and polymer (p-BDT-DPP) systems knowing that bisthiophene-2,5-Dihydropyrrolo[3,4-c]pyrrole-1,4-dione (DPP) has a low lying triplet energy level, which is further confirmed by Time-Dependent Density Functional Theory (TD-DFT) calculations. TD-

DFT and natural transition orbital (NTO) analysis were conducted to gain insight into the photophysical properties and features of excited states in $BDT(DPP)_2$, respectively. Femtosecond and nanosecond transient absorption spectroscopy were used to investigate the excited state kinetics in the synthesized compounds. A global target analysis (GTA) was also applied to help analyze the transient absorption data and identify the individual features. Fast formation of triplet pairs in thin film of p-BDT-DPP and $BDT(DPP)_2$ and the equilibrium formation of correlated triplet pairs and S_1 from triplet-triplet annihilation in solution of $BDT(DPP)_2$ is evidence of SF in these compounds. The short triplet lifetime, as a result of fast biexcitonic recombination pairs, provides additional support for their formation through singlet fission.

1. Introduction

Singlet fission (SF) is a spin-allowed process in which absorption of one photon in an assembly of two nearby chromophores forms two triplet excitons from an excited singlet.[1] It can be observed under favorable energetics when the energy of the first singlet state ($E(S_1)$) is at least twice that of the corresponding first triplet ($2\times E(T_1)$).[2-3] The first report of singlet exciton fission dates back to 1965 where it was proposed to explain the photophysics of anthracene crystals.[4] SF has attracted great attention in recent years as it has the potential to increase the maximum efficiency of solar cells from the Shockley-Queisser limit of 32% to nearly 45%.[5-6] To exceed the single junction limit, two charge carriers must be extracted from each triplet excitation generated through SF[7].

High triplet population efficiencies and long triplet-state lifetimes make singlet fission particularly attractive for practical applications. SF has been reported in a limited number of systems such as polyacenes[8-9], oligophenyls[10], diphenylisobenzofuran,[11] carotenoids,[12-13] conjugated polymers,[14-15] and dimers.[16-17] Although the range of compounds capable of undergoing singlet fission continues to grow, a highly efficient system incorporated into real photovoltaic applications remains to be discovered[18] with only limited literature reports of SF materials that have been successfully incorporated into a solar cell[19]. Furthermore, a detailed understanding of the SF mechanism remains obscure.

In most of the existing systems, the singlet fission mechanism is *inter*molecular in which the initial singlet state shares its energy with a neighboring chromophore and this leads to the formation of two triplets on adjacent molecules.[20] The formation of a bimolecular excimer in these systems is a limiting step because of its intermolecular nature, and it requires strong electronic coupling between the nearest neighbors.[21] A potentially more attractive alternative is to promote multiexciton generation based on *intra*molecular processes, in which two triplet excitons are generated in the same molecule. The fission in these systems is less dependent on molecular orientation and does not require intermolecular coupling.[22-23] Intramolecular singlet fission (iSF) has been observed in some conventional conjugated polymers and dimers but the yields to date have not exceeded 30%.[24-25] Recently, highly efficient iSF has been reported in polytetracene, polypentacene and electron donor-acceptor polymers.[20, 22, 26-28] The key requirements for iSF in these systems are: the triplet state energy should be close to half of the photoexcited singlet energy level[2]; and a significant charge transfer character should exist to facilitate the SF process[29].

Singlet fission can be achieved through two mechanisms:[30] (i) coupling the first singlet state (S_1) directly to the correlated triplet state (TT), which is a two electron process, or (ii) coupling these two states via a charge transfer state, which is achieved through two consecutive one-electron processes. It has been demonstrated that the second coupling is stronger than the first resulting in the charge transfer state playing a significant role in the singlet fission process.[31-32]

The following kinetic model was proposed from previous experimental and numerical simulations studies[1]:

$$s_1 + s_0 \rightleftharpoons (TT)^1 \rightleftharpoons T_1 + T_1 \quad (1)$$

This accepted model describes the conversion of an excited and ground singlet state to an intermediate state known as the correlated triplet pair which plays an important role in the SF process. The intermediate state subsequently converts into two independent triplet excitons. Recent advances in ultrafast spectroscopy make it possible to observe the intermediate steps in more detail. To date there is very little information about the dynamics of the correlated triplet pair[33]. However, this intermediate state is crucial in mediating SF as it is an overall singlet state[7] so investigating its dynamics can help understanding more about the mechanism of SF.

Exploiting molecular design based on the intramolecular donor-acceptor approach allows variation of the electron withdrawing building block to be used to tune the singlet energy level relative to the triplet energy level to meet SF energy level requirements. This molecular design leads to a new series of compounds capable of singlet fission for third generation optoelectronic devices. For inclusion in organic solar cell devices, it is also

desirable that the SF material can be solution processed, and in addition promote singlet fission in the solid state. This is important as many of the recent studies on SF materials have been carried out in solution and either studies in the solid state have not been undertaken or the materials do not show SF in the solid state.[22, 34]

Bisthiophene-2,5-dihydropyrrolo[3,4-c]pyrrole-1,4-dione (DPP)-based systems have recently demonstrated singlet fission with high yield.[35-37] Due to its polyene character, DPP exhibits a low-lying triplet excited state and so is a promising structure upon which to base new molecules for singlet fission applications.[38] In this work we describe the development of a solution processable, solid state SF material where we have combined 4,8-bis(5-(2-ethylhexyl)-4-hexylthiophen-2-yl)benzo[1,2-b:4,5-b']dithiophene (BDT) as the strong electron donor and DPP as the electron acceptor with low triplet energy level, to synthesize the molecule ($BDT(DPP)_2$) and a corresponding polymer (p-BDT-DPP). TDA-DFT (Time-Dependent Density Functional Theory with the Tamm-Dancoff Approximation)[39] and NTO (natural transition orbital) calculations were performed and confirmed the possibility of singlet fission in terms of the energetic landscape. We investigated singlet fission in both the molecule and polymer in the solid state and in solution. We report singlet fission in $BDT(DPP)_2$ in solution and in a thin film, and p-BDT-DPP in a thin film, with triplet yield of 20% and 80%, respectively.

2. Results

2.1. Structural and electronic properties

TDA-DFT (with the CAM-B3LYP[40] functional approximation to take into account possible CT excitations) and NTO analyses were conducted to gain insight to the photophysical

properties and features of excited states in $BDT(DPP)_2$, respectively. The optimized structure of $BDT(DPP)_2$ is shown in **Figure S1** and its coordinates are reported in the **Table S1** supplementary information. The thiophene ring, which is attached to the BDT core, is twisted at an angle of 44° relative to the BDT core, whereas the backbone structure is coplanar. The lowest-lying singlet excited state (S_1) is strongly dipole-allowed (f=1.73) with the vertical excitation energy of 2.24 eV. Moreover, the first triplet excited state (T_1), which is a dark state, has the vertical energy of 1.15 eV. It is found that for this compound and chosen level of theory HOMO→ LUMO excitation acts as the main configuration. The electron and hole NTO patterns for the S_1 and T_1 states, and the distribution patterns of the highest occupied molecular orbital (HOMO) and the lowest unoccupied molecular orbital (LUMO), are demonstrated in Figure 1. It was demonstrated that the splitting between singlet and triplet is proportional to the exchange integral $K_{HOMO,LUMO} = K_{hl}$ which is the repulsion of two identical overlap charge densities, defined by the product of HOMO (h) and LUMO (l).[1] The important factor for the K_{hl} is the degree to which the HOMO and the LUMO avoid residing on the same atoms. As a result, the large degree of spatial overlap between HOMO and LUMO supports the large singlet and triplet energy gaps and the electrons are delocalized over the whole molecule in which the LUMO is mostly located on the electron rich nitrogen and sulfur atoms. The exciton wave function in the electron and hole NTOs for the S_1 state has large overlap similar to HOMO/LUMO patterns. As a result, the S_1 state in $BDT(DPP)_2$ has a mixture of LE/CT character. On the other hand, the NTO electron and hole pairs of the T_1 state are localized within the DPP unit so the T_1 state of $BDT(DPP)_2$ is characterized dominantly by LE character. Therefore, the energies of such LE states are not influenced by $\Delta E_{H-L,}$ whereas the excitation energy of the S_1 state is directly

influenced by ΔE_{H-L}. Knowing this fact can assist the design of new structures with optimized energy levels.

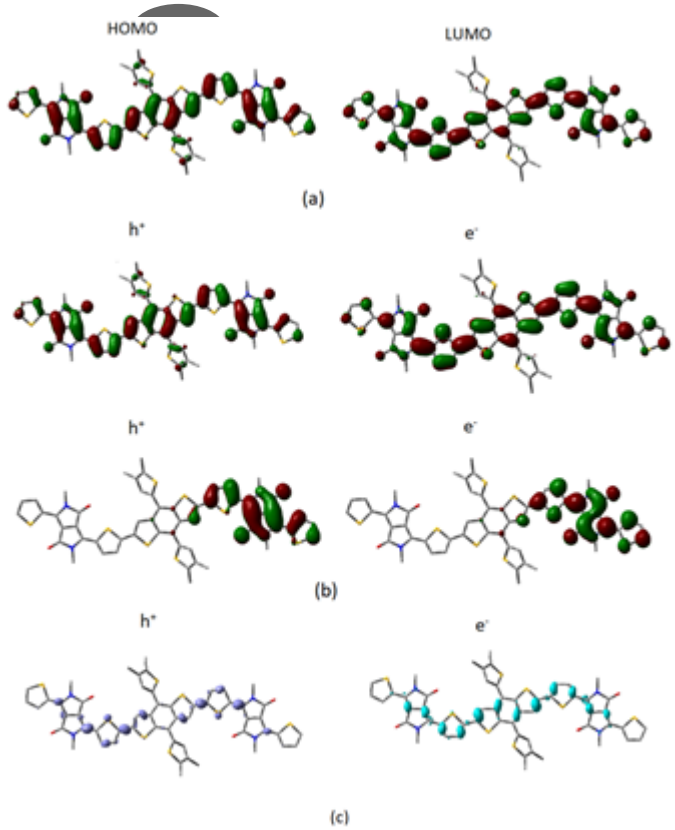

Figure 1. (a) Representation of the highest occupied molecular orbital (HOMO) and lowest unoccupied molecular orbital (LUMO), (b) NTO electron and hole pairs for the S_1 state (middle) and T_1 state (bottom) and (c) negative (right) and positive (left) difference densities of $BDT(DPP)_2$.

It has been reported in several organic chromophores including pentacene, push-pull polymers, diketopyrrolopyrrole and diphenylisobenzofuran, that charge transfer (CT) states play an important role in mediating the singlet fission process.[22, 36, 41-42] It was demonstrated that fast singlet fission needs the contribution of a CT-state, either through a singlet state with strong CT character or a virtual state.[33, 36, 43] Also, the amount of CT

character of the excited state affects the singlet-triplet energy level splitting. Therefore, we investigated the CT character of the first excited state for BDT(DPP)$_2$ and the results are summarized in Table S2 in the supplementary information. The results show a smaller charge transfer distance for BDT(DPP)$_2$ compared to DPP[44], and also confirms that the S_1 state has a mixture of LE/CT character. Another of the main requirements for a compound to undergo SF is that the energy of the first triplet state of the molecule is less than or at least equal to half of the first singlet state energy level. In addition, we can deduce the mixed LE/CT character from inspection of the difference densities between the S_0 and S_1 states as shown in Fig. 1 c). While this figure clearly indicates that there must be partial LE character, we can qualitatively see the partial CT character for this state from additional TDA-DFT calculations with a functional approximation that is known to severely underestimate CT transitions, namely B3LYP.[45-47] TDA-B3LYP, when applied with the same basis set as before, predicts the S_1 state to be red-shifted by nearly 0.5 eV (excitation energy of 1.76 eV). If the transition was a conventional local valence excitation, we would expect a red-shift of about 0.15 eV between both methods.[48]

To conclude, based on our calculations, the triplet energy level for BDT(DPP)$_2$ (T_1=1.15 eV) is nearly half of the first singlet excited state energy (S_1=2.24 eV). These theoretical results suggest that BDT(DPP)$_2$ is a potential candidate for SF.

2.2. Optical and electrochemical properties

The steady state absorption and fluorescence spectra of BDT(DPP)$_2$, p-BDT-DPP, DPP and BDT in chloroform solution and in thin films are shown in Figure 2A-D. BDT shows a sharp absorption peak at 405 nm and a broad absorption band in the region of 500-700 nm, Figure

2A. The compounds p-BDT-DPP, $BDT(DPP)_2$ and DPP each show two absorption bands in solution with maxima positioned respectively at about 750, 620 and 550 nm for the low energy band, and 435, 385 and 340 nm for the high energy band, see Figure 2A. The high energy band is attributed to a π-π^* transition and the low energy band is ascribed to the HOMO → LUMO $\pi \rightarrow \pi^*$ intramolecular charge transfer (ICT) transition between the donor and acceptor. There is a slight red shift in the absorption and fluorescence spectra of $BDT(DPP)_2$ by decreasing the polarity of the solvent, Figure S4, which suggests some charge transfer character of the lowest energy optical excitation, which is also well characterized for DPP-based molecules in several reports.[49-51] The absorption and fluorescence profiles of $BDT(DPP)_2$ show a bathochromic shift compared to BDT and DPP in both solution and thin film, which is the result of the intramolecular charge transfer process between BDT and the DPP unit. In addition, the polymer of BDT-DPP displays a large (~150 nm) red-shifted, broad absorption spectrum in both solution and thin film and a red-shifted fluorescence in comparison to $BDT(DPP)_2$ as a result of the -A-D-A-D- type structure. A new red-shifted feature appears in the absorption profiles of $BDT(DPP)_2$ and DPP in thin films, which is more distinct for $BDT(DPP)_2$. Also, there is a large bathochromic shift in the fluorescence of $BDT(DPP)_2$ and DPP in the thin films compared to the solution suggesting the formation of J aggregates in the solid state. The absorption spectrum of p-BDT-DPP in the solution of chloroform shows fine vibronic structures with resolved 0–0 and 0–1 peaks, similar to the absorption spectrum of the film and there is no spectral shift between solution and solid state absorption spectra. These results show that the p-BDT-DPP aggregates strongly in solution just as in the film. This behavior was already observed for other D–A copolymers[52-53] as a result of the high planarity and rigidity of the backbones and it means that even in

solution the chains do not lose their conjugation length and their π–π stacking. To investigate this phenomenon in more detail, we performed a temperature dependent UV-vis absorption measurement in chloroform solution, Figure S5. The results show that interchain interactions decrease and copolymer chains are allowed to separate at higher temperature.

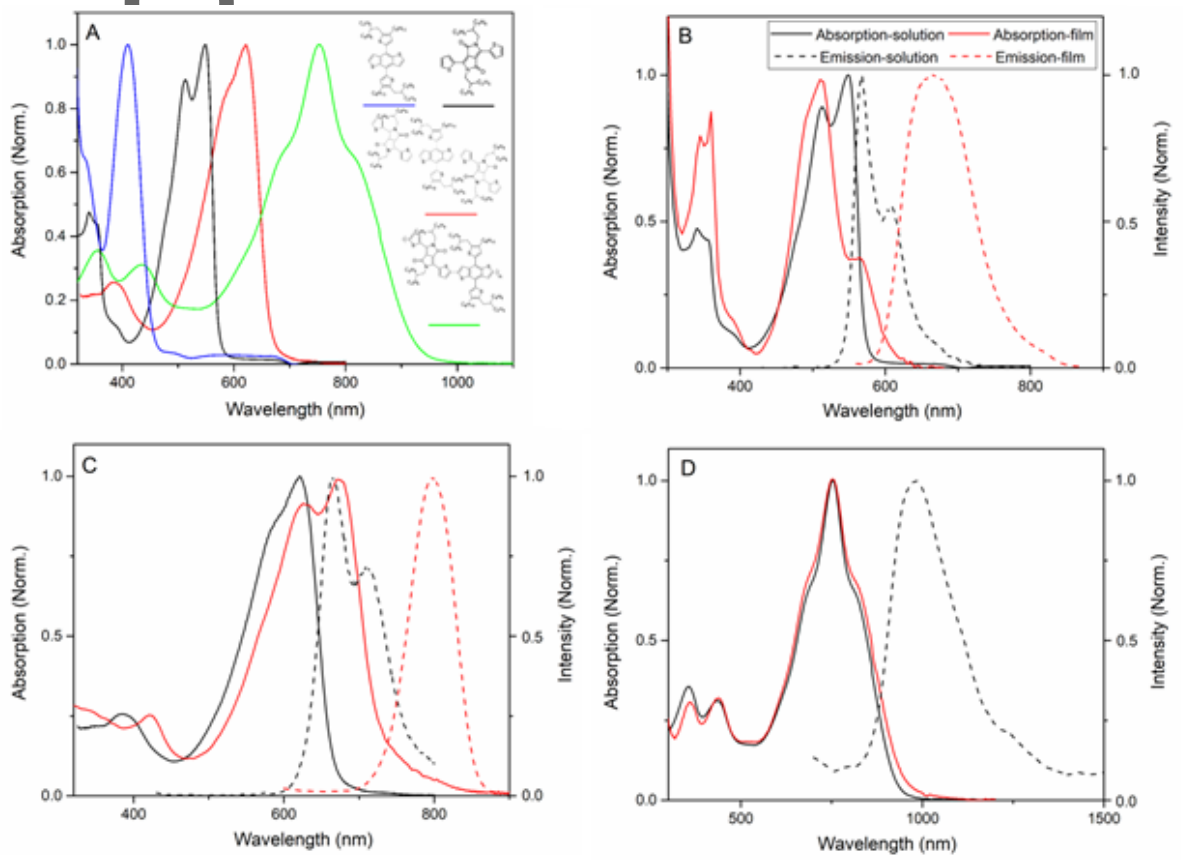

Figure 2. (A) Absorption spectra of $BDT(DPP)_2$, p-BDT-DPP, DPP and BDT in solution of chloroform and absorption and fluorescence spectra of (B) DPP, (C) $BDT(DPP)_2$ and (D) p-BDT-DPP in chloroform solution and thin film.

The fluorescence of p-BDT-DPP is significantly quenched in the thin film to such a degree that the fluorescence spectrum could not be determined. This may suggest that a new

pathway exists for singlet state quenching in the polymer in the solid state. The optical bandgaps of $BDT(DPP)_2$, p-BDT-DPP and DPP in solution and the solid state are calculated from the onset of absorption (Figure 2A-D) and are summarized in Table S3 in the supplementary information.

To observe the phosphorescence of a purely organic compound, the radiative rate of phosphorescence should outcompete the non-radiative rate. To meet this criterion, spectroscopy at cryogenic temperature (77 K) is required.[54-56] The emission of $BDT(DPP)_2$ in 2-methyl-tetrahydrofuran (m-THF) at room temperature and 77 K in the spectral area of 1000-1500 nm (with >1200 nm highpass filter) is shown in Figure S2. By decreasing the temperature to 77 K, the non-radiative loss pathways are frozen out [57], and a peak appears at about 1300 nm (0.95 eV) which is assigned to emission from the triplet state. This suggests that $BDT(DPP)_2$ in solution matches the energy level requirement for SF, that is, the triplet energy (0.95 eV) is close to half of the singlet energy level (1.88 eV).

An estimate of the absolute energy levels against vacuum can be determined from cyclic voltammetry and the cyclic voltammograms of $BDT(DPP)_2$, p-BDT-DPP and DPP are shown in Figure S3. The HOMO and LUMO energy levels and the electrochemical bandgaps of $BDT(DPP)_2$, p-BDT-DPP and DPP are estimated from the onsets of the oxidation and reduction peaks and are summarized in Table S3.

2.3. p-BDT-DPP excited state dynamics in solution and thin films

The polymer p-BDT-DPP was designed based on the donor-acceptor interactions in a polymer chain and appears to be strongly aggregated in solution. Femtosecond transient absorption (TA) measurements were used to probe the dynamics of excited states in this

compound. The TA spectra in the NIR region and kinetic traces at selected wavelengths of p-BDT-DPP, following excitation at 630 nm in both solution and thin film, are shown in Figure 3A-D. In solution, a ground state bleach (GSB) in the region of 800-900 nm and a broad photoinduced absorption (PIA1) in the 900-1250 nm region, are observed in the TA spectra, with similar but mirrored kinetics (see Figure 3C). After 100 ps, there is no detectable TA signal in either region indicating that the exciton generated from photoexcitation of p-BDT-DPP decays quickly to the ground state with a ~10 ps time constant without forming any long-lived intermediates. On the other hand, the TA spectra (Figure 3B) of the thin film show a GSB in the 850-960 nm range and a broad positive absorption signal (PIA1) in the 960-1250 nm region. In contrast to the solution, the PIA1 and GSB features are still observed at delay times of 300 and 850 ps in the thin film (Figure 3D). Comparing the excited state kinetics of p-BDT-DPP in solution and film at 1100 nm, see Figure 3D, indicates the formation of a long-lived feature. As shown in Figure 3D, the decrease in ΔA of the $S_1 \rightarrow S_n$ absorption band follows the growth of another feature on a time scale of about 100 ps suggesting that PIA1 in the film sample comprises the overlap of more than one feature which is confirmed by other evidence discussed below.

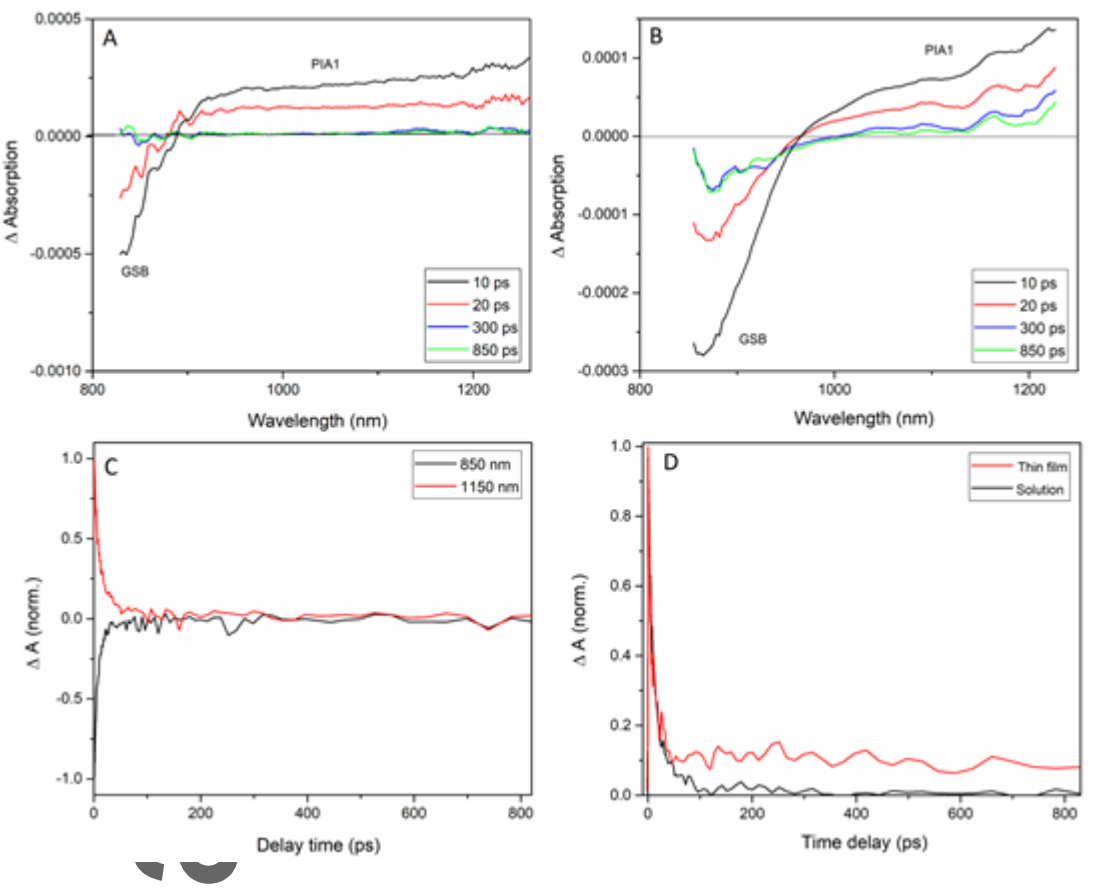

Figure 3. Transient Absorption spectra of p-BDT-DPP in a chloroform solution (A),and in thin film (B) at a time delays of 10, 20, 300 and 850 ps; kinetic traces of p-BDT-DPP at 850 nm and 1,150 nm in chloroform solution (C), and 1150 nm in solution and thin film (D). The solution and thin film of p-BDT-DPP were excited at 630 nm with a fluence of 10 μJ/cm^2.

To find more detail about the kinetics of the long-lived species in p-BDT-DPP in thin film, we have conducted nanosecond transient absorption (ns-TA) measurements with excitation at 630 nm. The kinetic trace at 1200 nm is shown in Figure S10. It shows a single exponential decay with the time constant of 150 ns.

In light of the fast decay of singlet excited state as indicative from Time-correlated single photon counting (TCSPC) at low temperature (Figure S6), the presence of a long-lived

species in the ns-TA measurement and non-exponential kinetics at 1150 nm in fs-TA (Figure 3D), a two species sequential model A → B → GS was assumed as the simplest model of p-BDT-DPP in the thin film. We tentatively assign species A to the S_1 state, which decays with a time constant τ_A=10 ps from the fast component in fs-TA and species B to the T_1 state that decays with a time constant of 150 ns from ns-TA.

The triplet sensitization technique has been used to find the triplet absorption spectrum and the molar extinction coefficient for triplet−triplet absorption. Palladium octaethylporphyrin (PdOEP) was chosen as the triplet sensitizer. Since PdOEP has two narrow and isolated absorption bands at 400 and 550 nm (Figure S7) and they both overlap with the absorption band of p-BDT-DPP, the sensitizer cannot be excited selectively. As a result, the sensitized transient absorption spectrum is a linear combination of the PdOEP, p-BDT-DPP triplet spectra, and the non-sensitized p-BDT-DPP spectrum. Thin film TA spectra of PdOEP show a narrow, negative ground state bleach (GSB) at 550 nm and no positive photoinduced absorption following excitation at 400 nm as shown in Figure S8. The kinetic traces of the sensitized and non-sensitized p-BDT-DPP films at selected wavelengths of 650 and 1100 nm are shown in Figure 4A and B, respectively. The population of the triplet state occurs at a time delay of about 100 ps, and is assigned to triplet energy transfer from the PdOEP to p-BDT-DPP. To find the triplet absorption spectrum, global target analysis was performed on p-BDT-DPP:PdOEP blend film (Figure S9). A global target analysis (GTA) was used to analyze the transient absorption data to help identify the individual features and their population variation with time.[22] GTA yields the associated spectra and concentration profile for S_1 and T_1, which are shown in Figure S9.

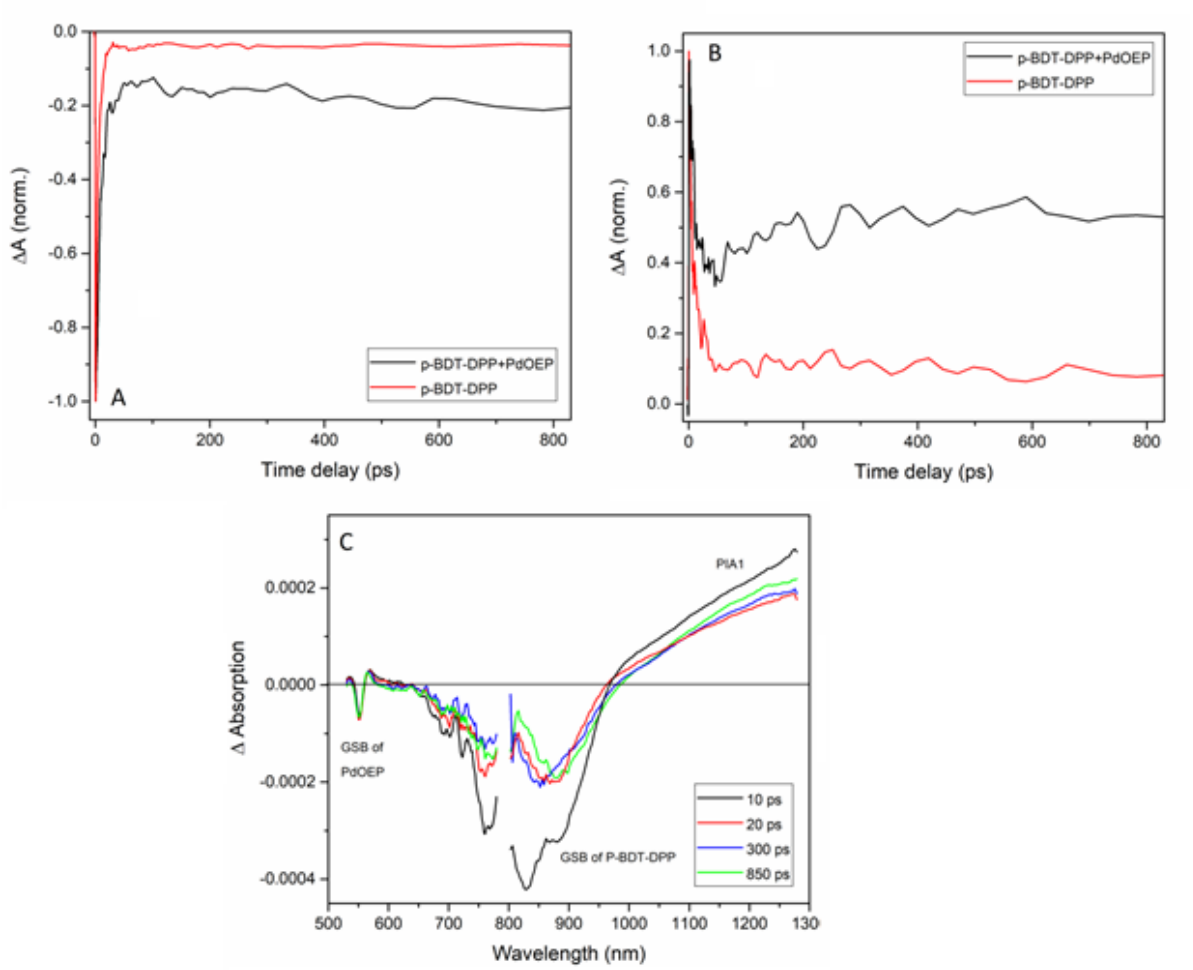

Figure 4. (A) and (B) Kinetic traces of p-BDT-DPP thin films with and without palladium octaethylporphyrin (PdOEP) as a sensitizer at 650 nm, and 1100 nm, respectively. (C) Transient absorption spectra of a p-BDT-DPP:PdOEP blend film for time delays of 10, 20, 300 and 850 ps, following excitation at 400 nm, with a fluence of 10 μJ/cm^2.

Fast triplet formation (<100 ps) in p-BDT-DPP films can be one piece of evidence for ruling out intersystem crossing (ISC) as the dominant mechanism of triplet formation, because ISC on such a short timescale is mostly observed in the systems with heavy atoms that facilitate spin orbit coupling, however, there are a few counterexamples in the literature.[22] To find more detail about the dynamics of the sensitizer-generated triplet species in p-BDT-DPP

films, we have conducted nanosecond transient absorption (ns-TA) measurements with excitation at 400 nm. The triplet state decay for the sensitized p-BDT-DPP film, monitored at 1200 nm, is shown in Figure S10. The best fit analysis indicates biexponential decay with time constants of about 130 ns and 2 µs, indicating two different triplet excited states in the p-BDT-DPP:PdOEP blend film. The longer lived triplet exciton is assigned to the single triplet species formed from the sensitization experiment and the shorter-lived component corresponds to the triplet pair that is generated from direct excitation of p-BDT-DPP, which matches with the results of ns-TA of pure p-BDT-DPP. A faster recombination rate for SF generated triplets would be expected for correlated triplet pairs resulting in an enhanced contribution of spin-allowed geminate triplet-triplet annihilation compared to the sensitizer generated single triplets, with a slower recombination rate. The results are strongly suggestive that singlet fission occurs in the thin film of p-BDT-DPP but not in aggregated solution although the ground state absorption spectra are similar in both solution and thin film. We believe that the singlet is very low in energy in solution, and the localized triplet states are not very strongly affected by the presence of many repeat units in the polymer, so the energy requirements of $2T_1<S_1$ are difficult to satisfy and inhibit singlet fission in solution.

2.4. BDT(DPP)$_2$ excited state dynamics in thin film

Ultimately, for inclusion into printed solar cells new SF materials must be solution processable and promote SF in the solid state. Therefore, solid state dynamics of BDT(DPP)$_2$ were examined using TA measurements on thin films of BDT(DPP)$_2$. TA spectra and kinetics of BDT(DPP)$_2$ after exciting at 630 nm, are shown in Figure 5A and B, respectively. A negative

ground state bleach (GSB) signal in the region of 520-740 nm, mirroring the steady state absorption and a broad positive photoinduced absorption (PIA1) in the near-infrared (NIR) region with maximum intensity at 1100 nm, appears at the first delay period of the measurement, Figure 5B. The shape of the PIA1 in the TA spectrum at a time delay of 600 ps is different from the spectrum at the earlier times, as shown in the inset graph of Figure 5A, suggesting that this broad peak comprises more than one overlapping excited state feature. To confirm this, a GTA was performed on the transient absorption data set of $BDT(DPP)_2$ in thin film using a sequential A → B → GS model. The associated spectra and concentration profile for A and B are shown in Figure 6. The spectrum of species B is very similar to that of the triplet absorption of $BDT(DPP)_2$, which is derived from the PdOEP-sensitized experiment and is discussed in more detail in the next section (Figure 7). As a result, we assigned A to the S_1 state, which decays in τ_A=85 ps, and B to the T_1 state that decays in τ_B=380 ps.

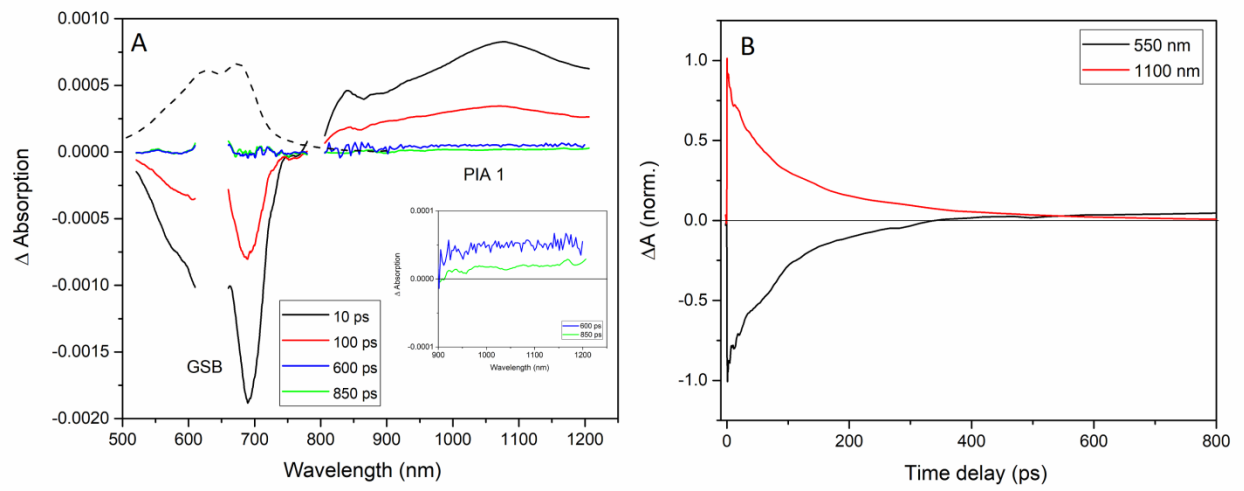

Figure 5. Thin film transient absorption measurement data for $BDT(DPP)_2$ with 630 nm excitation at 10 μJ/cm^2. A) Spectral slices at 10, 100, 500 and 850 ps, the steady state absorption (dashed line) is also shown for comparison, and B) kinetic traces of the GSB and PIA1.

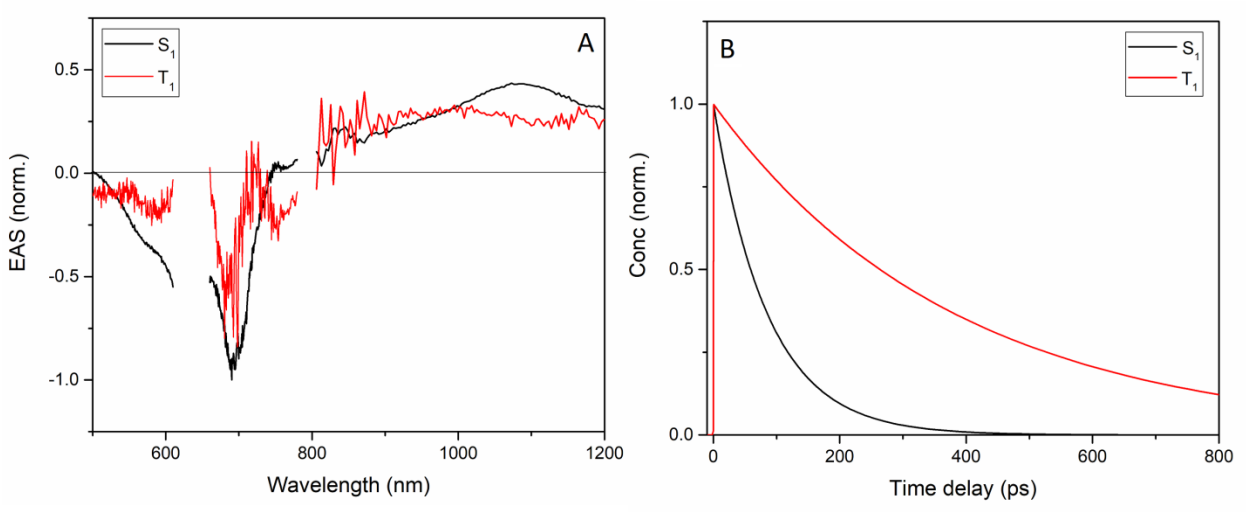

Figure 6. (A) The associated spectra and (B) concentration profile versus time for S_1 and T_1 from the global target analysis for $BDT(DPP)_2$ in thin film.

To confirm the assignment of species B from the GTA as a triplet, the triplet sensitization technique has again been used. Before performing time-resolved measurements, the steady state emission of PdOEP in the presence of $BDT(DPP)_2$ was investigated to find out more about triplet energy transfer. A Stern-Volmer quenching plot of the sensitizer (PdOEP), see Figure S11, indicates a decrease of the phosphorescence of the sensitizer (PdOEP) by increasing the concentration of $BDT(DPP)_2$, suggesting triplet energy transfer from the sensitizer to $BDT(DPP)_2$. Finally, TA experiments were performed for PdOEP sensitized $BDT(DPP)_2$ thin films (60:40 weight ratio) to find the triplet absorption spectrum and the lifetime of generated triplets. The kinetic traces of the sensitized and non-sensitized $BDT(DPP)_2$ films at 650 and 1100 nm are shown in Figure 7A and B, respectively. In the $BDT(DPP)_2$:PdOEP blend film, the kinetic trace of the GSB shows that the excited state of $BDT(DPP)_2$ is being repopulated on timescales exceeding 300 ps attributed to triplet exciton energy transfer from the PdOEP to $BDT(DPP)_2$. The same trend is observed in the dynamics

of the positive peak centered at 1100 nm when $BDT(DPP)_2$ is sensitized showing the repopulation of triplet state in that system. The thin film TA spectra for $BDT(DPP)_2$ in the presence of PdOEP following excitation at 400 nm are shown in Figure 7C for different time delays. The broad, positive photoinduced absorption peak in the near-infrared (NIR) region in the neat BDT-DPP_2 decays to zero within 850 ps film whereas in the photosensitized experiment the signal at 1100 nm is still present at longer times, which is assigned to the triplet ($T_1 \rightarrow T_n$)-induced absorption arising from triplet generation on $BDT(DPP)_2$ due to sensitization from PdOEP. As previously mentioned, the sensitizer cannot be excited selectively, so the sensitized TA spectrum is a linear combination of the PdOEP, $BDT(DPP)_2$ triplet spectrum, and the PdOEP sensitized $BDT(DPP)_2$ spectrum. As there is no TA signal at a time delay of 800 ps for either $BDT(DPP)_2$ thin films (Figure 5), or PdOEP, any positive photoinduced absorption band of the PdOEP sensitized $BDT(DPP)_2$ thin film at time delay of 800 ps can be associated with triplets on $BDT(DPP)_2$ generated via sensitization (Figure 7D). The associated spectrum of species B from the GTA is similar to the triplet induced absorption from the sensitization technique as shown in Figure 7D. The spectral agreement of the T_1-induced absorption spectra from the sensitization experiment and the second excited state from GTA suggests that triplets are being generated on an ultrafast time scale following the excitation of the $BDT(DPP)_2$ in the solid state. As discussed above, the fast triplet formation (<100 ps) supports ruling out ISC as the main mechanism of triplet formation in $BDT(DPP)_2$.

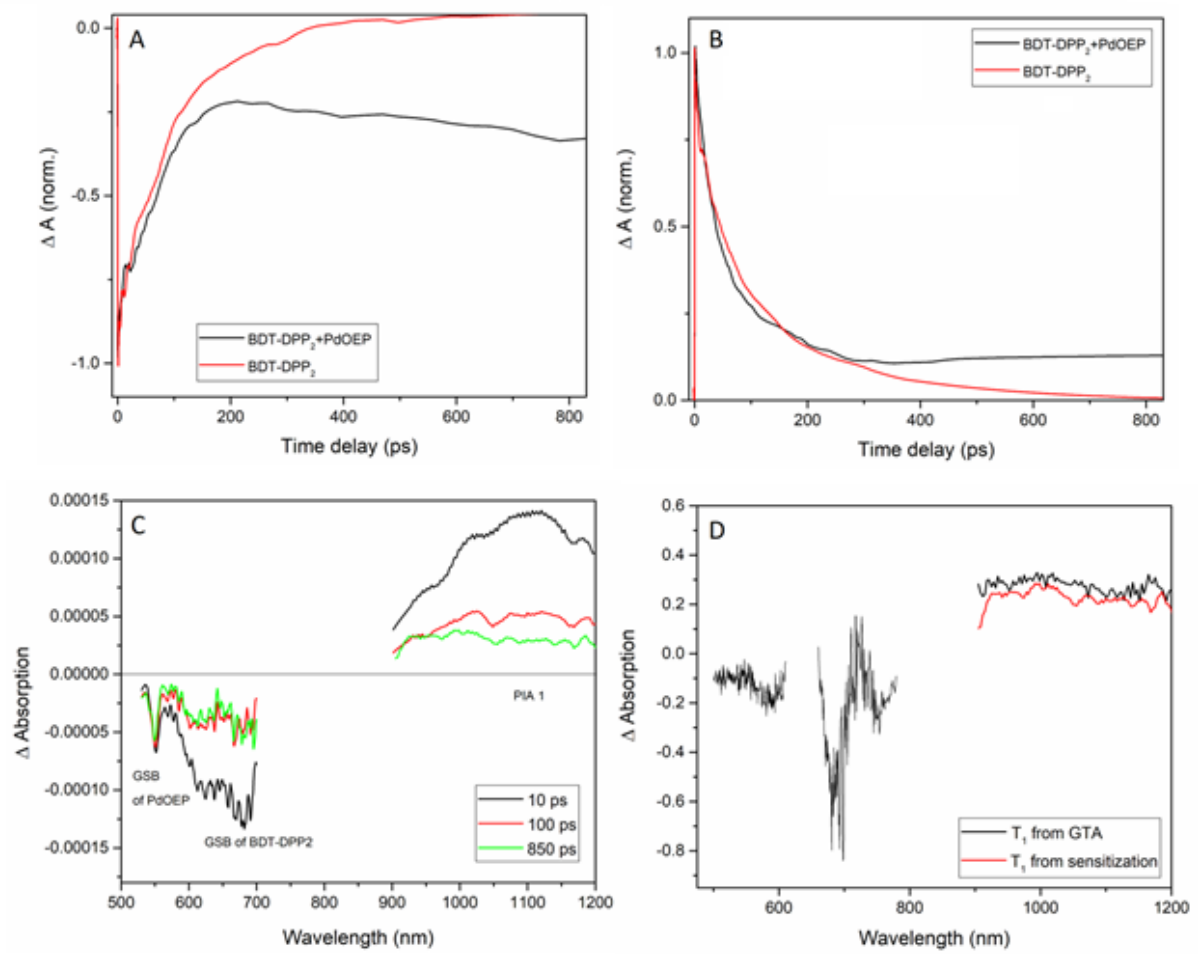

Figure 7. (A, B) Kinetic traces of sensitized and non-sensitized thin films of $BDT(DPP)_2$ for selected wavelengths of (A) 650 nm and (B) 1100 nm, (C) TA spectra of thin film sensitized $BDT(DPP)_2$ for time delays of 10, 100 and 850 ps after exciting at 400 nm at 10 μJ/cm^2 and (D) T_1-induced absorption spectrum of the $BDT(DPP)_2$ derived from triplet sensitization technique and associated spectrum of 2nd excited state species from GTA.

To further investigate the dynamics of the triplet feature in the sensitized $BDT(DPP)_2$ film, we have conducted ns-TAS measurements for the $BDT(DPP)_2$: PdOEP blend film excited at 400 nm, and monitored the triplet state decay at 1050 nm, see Figure S12. In the sensitized experiment, the generated triplets on the sensitizer are transferred to the organic

chromophore and form isolated triplets.[34] The isolated triplets formed via photosensitization have a single, long lifetime of 2.2 μs compared to the lifetime of the triplets generated in the $BDT(DPP)_2$ alone film (about 1 ns). This fact suggests the formation of the triplet pair in $BDT(DPP)_2$ thin films is via singlet fission (SF), and the faster recombination rate of triplet pairs compared to the isolated triplets may be due to the enhanced contribution of spin-allowed geminate triplet-triplet annihilation rather than the slower recombination of isolated triplet excitons. The results are strongly suggestive that the triplet pairs are formed via SF in thin film.

2.5. $BDT(DPP)_2$ excited state dynamics in dilute solution

One remaining question is whether the SF in $BDT(DPP)_2$ is inter- or intramolecular. We have examined the excited state dynamics of $BDT(DPP)_2$ in a dilute chloroform solution (10 μM), to reduce possible bimolecular interactions. Selected fsTA spectra and extracted kinetic traces of $BDT(DPP)_2$ after exciting at 630 are shown in Figure 8A and B respectively. A negative ground state bleach (GSB) signal in the region of 520-690 nm is seen in the TA spectra, mirroring the steady state absorption, along with a negative stimulated emission (SE) peak at 690-780 nm that corresponds to the $BDT(DPP)_2$ fluorescence. Also, a broad positive photoinduced absorption (PIA1) in the near-infrared (NIR) region with maximum intensity at 1100 nm appears at the first delay time. A second photoinduced absorption (PIA2) at 550 nm, strongly overlapping the GSB, is also observed and grows in with the decaying of PIA1, Figure 8B. The kinetic trace of this signal, a mix of the decreasing GSB and increasing PIA2, shows that it changes from negative to positive ΔA at about 400 ps. The steady state absorption and emission spectra of $BDT(DPP)_2$ are also plotted for comparison

with the GSB and SE signals, Figure 8A. According to the kinetic traces at the selected wavelength of 570 and 710 nm, the GSB and SE signals decay at different rates indicating that the first excited state (S_1) populates another excited state, i.e. the TA data of $BDT(DPP)_2$ in dilute solution comprises the overlapping of more than one excited state features, confirmed by global target analysis discussed below.

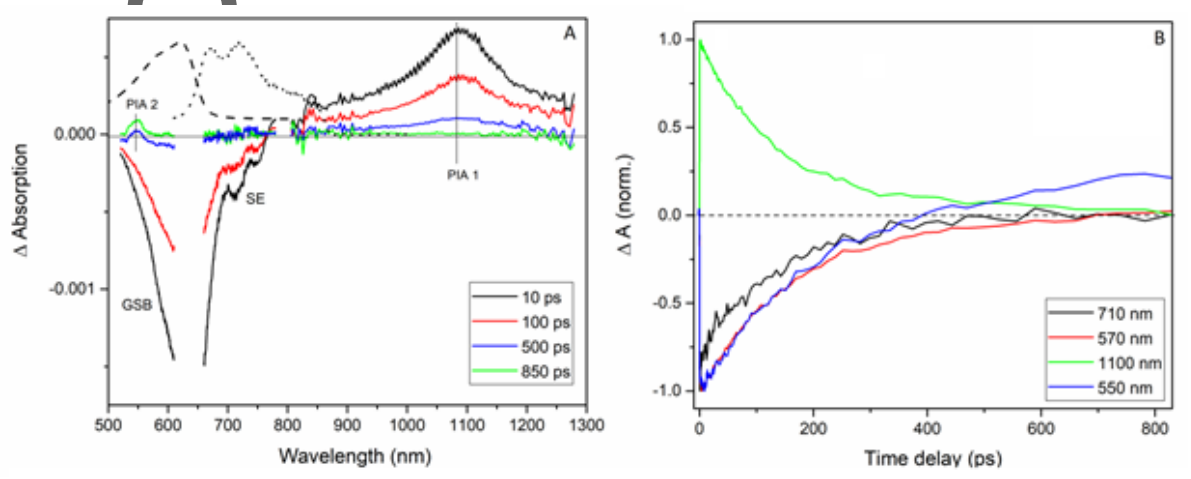

Figure 8. Transient absorption measurement data for $BDT(DPP)_2$ in dilute solution of chloroform with 630 nm excitation at 10 μJ/cm^2. A) Spectral slices at 10, 100, 500 and 850 ps, the steady state absorption (dashed line) and fluorescence (dotted line) are also shown for comparison, and B) kinetic traces at selected wavelengths of 550, 570, 710 and 1100 nm.

To further characterize the excited states in a dilute solution of $BDT(DPP)_2$, TA measurements were performed in a series of solvents with different polarities. The kinetic traces of PIA1 for $BDT(DPP)_2$ in cyclohexane, dichloromethane and chloroform are shown in Figure S13. There is no polarity dependence on the decay kinetics of the PIA1 at 1100 nm, suggesting the lack of charge transfer character in this state.

We performed a global analysis on the transient absorption data of BDT(DPP)$_2$ in dilute solution using a two-species model (A → B → GS). The associated spectra and concentration profiles versus time for the A and B features are shown in Figure 9A and B. The first component is ascribed to the photogenerated singlet exciton which has a lifetime of about 50 ps according to target analysis. The first singlet exciton forms species B with a rate (K_{SF}) of k=0.019 ps^{-1}, which subsequently decays with a rate (K_{TT}) of 0.006 ps^{-1}. Species B has different transient absorption spectrum to that of the PdOEP-sensitized triplet absorption of BDT(DPP)$_2$ (Figure 7D) at short wavelengths. By looking closer at the fitted model, we found that the residual spectrum at time delays greater than 600 ps is very similar to the absorption from the S_1 state. According to the literature,[58-60] the vibronic progression of the isolated triplet transition might be different from the triplet-pair state resulting in a different absorption spectrum. As a result, we assign species B as a correlated triplet-pair (T_1T_1) state that results from SF equilibrium. We proposed the model shown in Figure 9C for BDT(DPP)$_2$ in dilute solution. In this model, the singlet exciton undergoes a spin-allowed internal conversion to an overall singlet, correlated triplet-pair state on the ps time scale. However, the evidence shows that this correlated triplet pair could not diffuse apart to form separated correlated triplets and they annihilate together to re-form the S_1 excited state. It was reported that chemical systems in which triplet exciton interactions are very strong and the triplet pair cannot spatially separate might yield only the interacting triplet pair.[7] This is clearly apparent in the short triplet-pair lifetimes reported in some systems such as conjugated polymers and covalently tethered molecular pairs.[59, 61] We assume that SF in BDT(DPP)$_2$ is of an intramolecular character and confinement of two triplet excitons on one molecule results in faster biexcitonic recombination rates. The results are strongly

suggestive that the triplet pairs are formed via SF in both solution and thin film of $BDT(DPP)_2$.

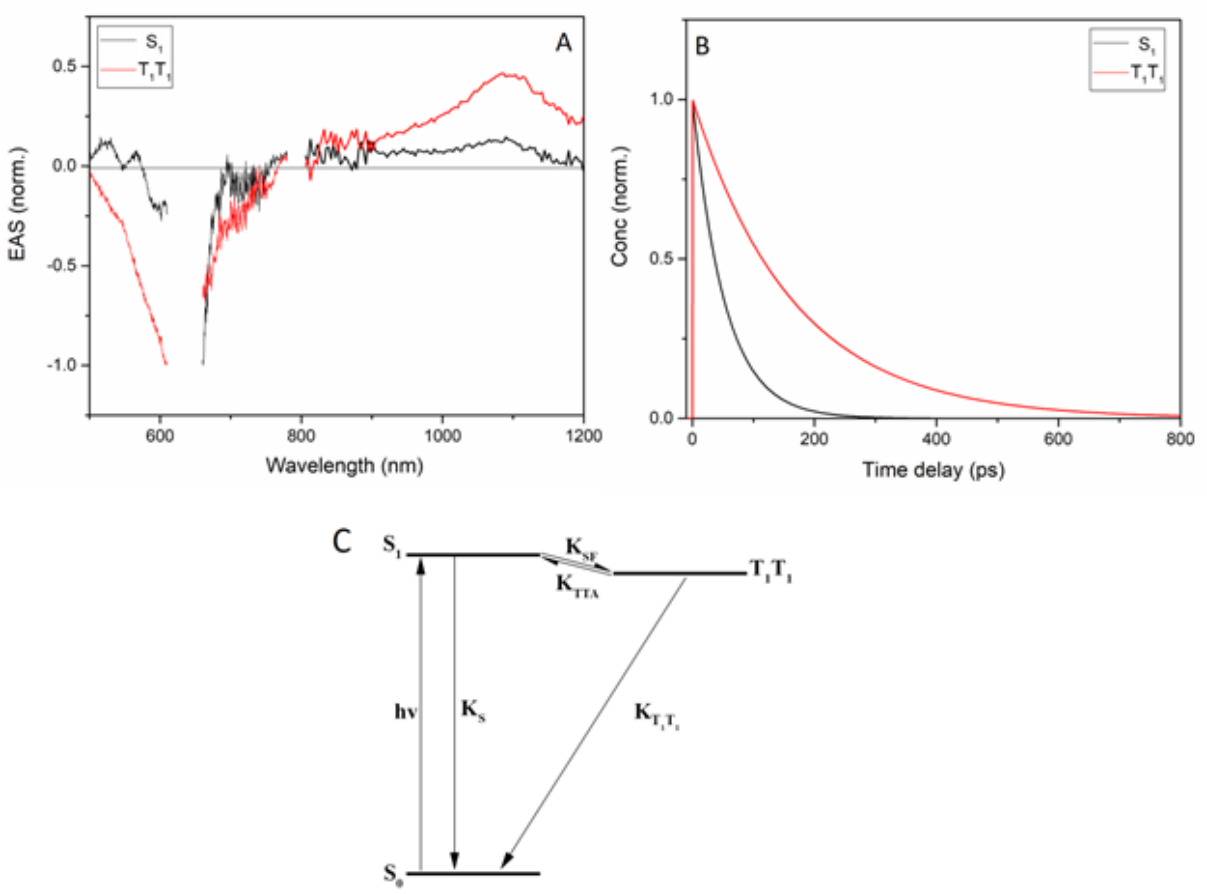

Figure 9. (A) The associated spectra and (B) concentration profile versus time for S_1 and T_1T_1 from the global target analysis for $BDT(DPP)_2$ in dilute solution and (C) Energy level schematic and kinetic model for SF dynamic in solution.

2.6. Determining the triplet yield

There are several common methods to calculate the triplet yield of singlet fission materials. One is calculating the number of molecules in the singlet state that are converted to the triplets by measuring the changes in the ground state bleach during the interconversion process, however this method is not very accurate for our system due to the large overlap

between singlet and triplet state absorption.[22] Another method is triplet sensitization in which a well-known triplet sensitizer such as PdOEP is used to transfer triplet energy to the triplet states of the molecule of interest and so the extinction coefficient for triplet-triplet absorption can be calculated.[62] The triplet concentration can then be determined from the magnitude of the TA signal and the triplet yield can be calculated. Using the triplet sensitization technique, it is determined that the triplet yields are 70% and 18% for p-BDT-DPP and $BDT(DPP)_2$ in thin film, respectively (more details in the Supplementary Information). Although $BDT(DPP)_2$ is believed to undergo SF in dilute solution, as indicated by the very short fluorescent time constant and formation of correlated triplet-pair (T_1T_1) state, no signal for triplet (T_1) are detected in the GTA. Therefore, the triplet yield cannot be determined. Also, in thin films of $BDT(DPP)_2$, the triplet yield calculation contains significant errors, as the $BDT(DPP)_2$ SF generated triplets have a short lifetime, undergo fast recombination, and the singlet and triplet absorption spectra of $BDT(DPP)_2$ have a large overlap. The triplet yields, single triplet and triplet pair lifetimes of P-BDT-DPP and $BDT(DPP)_2$ in solution and the solid state are summarized in Table 1. The results suggest that $BDT(DPP)_2$ undergoes singlet fission in both dilute solution and thin film and p-BDT-DPP shows singlet fission only in the thin film. However, p-BDT-DPP has a higher singlet fission yield and longer triplet pair lifetime in the thin film compared to $BDT(DPP)_2$.

Table 1. The triplet yields, isolated triplet and triplet pair lifetimes of p-BDT-DPP and $BDT(DPP)_2$ in dilute solution and thin film.

Sample	Triplet pair lifetime (ns)	isolated triplet lifetime(μs)	SF yield

p-BDT-DPP in film	150	2	70%
p-BDT-DPP in solution	-	-	NO SF
BDT(DPP)$_2$ in solution	-	-	Cannot be determined
BDT(DPP)$_2$ in film	~1	2.04	18%

3. Discussion

The results indicate that triplet pairs are formed in BDT(DPP)$_2$ in thin film through SF as shown in Figure 10B. The evident also shows that correlated triplet pairs are formed via SF in a single chromophore of BDT(DPP)$_2$ in solution but they did not diffuse apart to form separated triplet pairs before recombination. The results show that SF mechanism is independent of intermolecular orientation and coupling, which is an indirect indication of intramolecular singlet fission (iSF). Also, the short lifetime of the triplet pairs and triplet-triplet annihilation provide additional support to the intramolecular nature of singlet fission in BDT(DPP)$_2$, as confinement of two triplet excitons on one molecule results in faster biexcitonic recombination rates. However, p-BDT-DPP shows SF only in thin film but not in solution although the ground state absorption spectra are similar in both solution and thin film as shown in Figure 10A. We believe that the singlet is very low in energy in solution, and the localized triplet states are not very strongly affected by the presence of many repeat units in the polymer, so the energy requirements of $2T_1<S_1$ are difficult to satisfy in the solution and that is why it is not undergo singlet fission in solution. There is a higher probability for efficient localization of the resulting triplets in well-separated polymer

chains, which would result in slower biexcitonic recombination rates suggesting why singlet fission is more efficient and the triplets live longer in the polymer sample. Besides, the triplets are separated in p-BDT-DPP resulting in slower biexcitonic recombination rates.

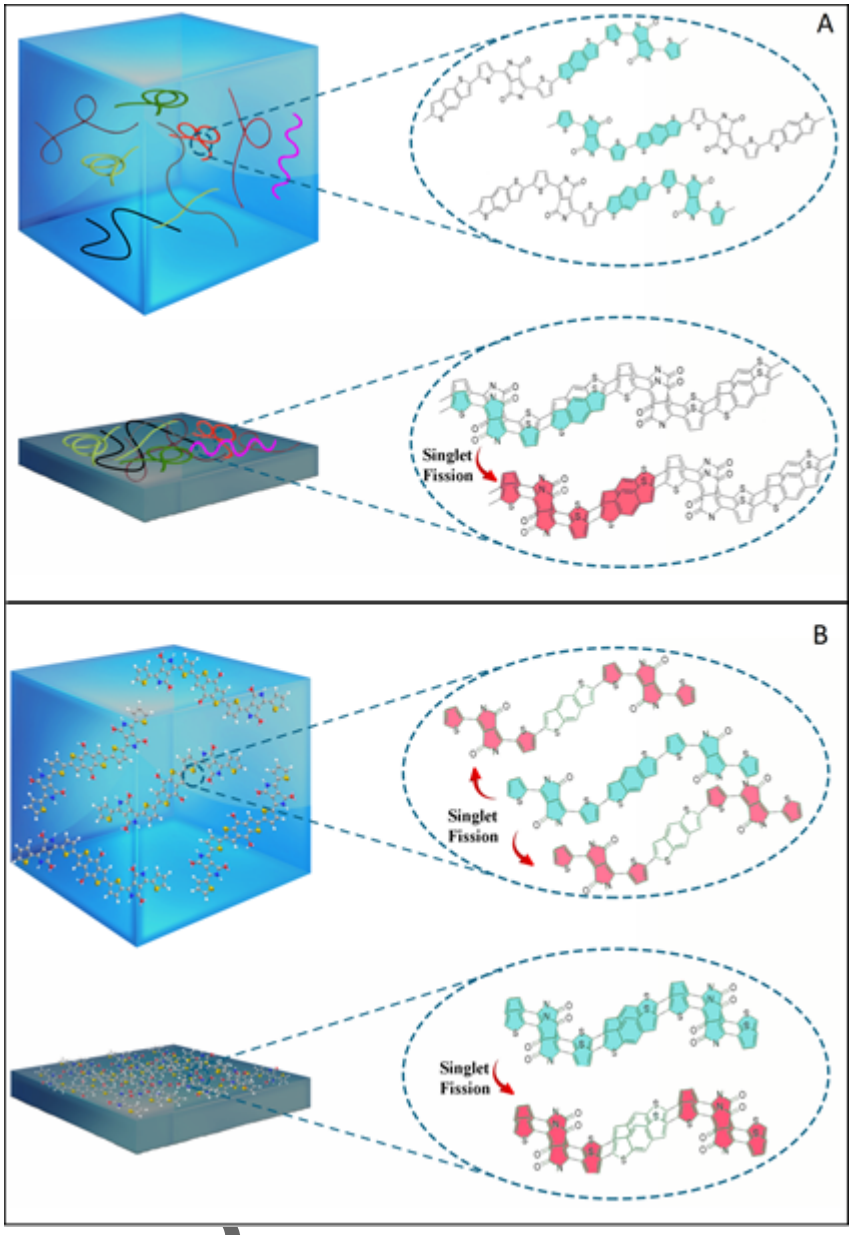

Figure 10. Cartoon of (A) Intermolecular singlet fission process where a singlet exciton (blue) splits into two triplet excitons (red) on neighboring molecules in aggregate form, (B)

Intramolecular singlet fission process where a singlet exciton (blue) splits into two triplet excitons (red) on the same chromophore in both solution and aggregate form.

According to Smith et al.[1], the best choice of chromophore for charge transfer mediated SF is through symmetric and direct linking of two chromophores when the link is planar. The charge transfer state can act as a real intermediate state in the incoherent transformation of the locally excited state (S_1) to the double triplet state (TT) and facilitate SF[1] so the acceptor-donor-acceptor module with linear backbone is a good candidate structure for designing new chromophores for mediated SF. However, the problem for such a system is that direct linking of two chromophores converts the two chromophores into a single chromophore that reduces the first singlet energy level (S_1) and might even lie below twice the energy of first triplet and make the SF endothermic. Thus, it is important to choose the right donor such that there is sufficient charge transfer for SF while keeping the singlet energy level higher than twice the energy of first triplet for exothermic SF. These considerations can assist towards new molecular designs with higher SF yield in future work. It is also shown that the distance between two triplets that are generated in one chromophore through the intramolecular SF process plays an important role so introducing a spacer between the donor and acceptor can result in separating the two triplet excitons resulting in longer lived triplets and more efficient SF.

4. Conclusion

Designing new compounds based on conjugating strong donor and acceptor building blocks provides a pathway for the generation of new materials capable of singlet fission suitable for optoelectronic devices. An organic molecule ($BDT(DPP)_2$) and polymer (p-BDT-DPP)

based on a donor-acceptor framework comprising benzodithiophene (BDT) as electron rich and bisthiophene-2,5-Dihydropyrrolo[3,4-c]pyrrole-1,4-dione (DPP) as electron deficient were designed, synthesized and investigated for singlet fission. TDA-DFT calculations show that the electrons and holes in the first singlet excited state of $BDT(DPP)_2$ are delocalized over the whole molecule and the first singlet excited state in $BDT(DPP)_2$ has a mixture of LE/CT character. However, the electron and hole NTOs of the T_1 state are localized within the DPP unit. It also shows that the first triplet excited state has the energy level of about half of the first singlet excited state. The steady state measurements also confirm that this compound meets the energy level requirement for singlet fission. The ns and fs transient absorption spectroscopy measurements were used to investigate the excited state kinetics in the synthesized compounds. Fast formation of the triplet state (<100 ps) in p-BDT-DPP in thin film suggests singlet fission is operating but there is no sign of triplet formation in the solution. On the other hand, singlet fission occurs in $BDT(DPP)_2$ in both thin film and in dilute solution suggesting that the SF mechanism is more probably intramolecular than intermolecular in this molecule. The results suggest the formation of correlated triplet pairs in a single chromophore of $BDT(DPP)_2$ but they did not diffuse apart to form well-separated triplet pairs. The triplet pair lifetimes and the triplet yields in p-BDT-DPP and $BDT(DPP)_2$ in thin film are about 150, 1 ns and 70% and 20%, respectively. The short lifetime of triplets in $BDT(DPP)_2$ provides additional support to the intramolecular nature of the singlet fission as confinement of two triplet excitons on one molecule results in faster biexcitonic recombination rates. The results of this work can lead to the development of a new class of SF materials for potential application in third generation optoelectronic devices.

5. Experimental methods

5.1. Material synthesis

The commercially available chemicals were purchased from Sigma-Aldrich, Boron Molecular, Matrix Scientific, Ajax Finechem, Univar, Luminescence Technology Corp. and Suna Tech Inc. and all chemicals were used as received. 4,8-Bis(5-(2-ethylhexyl)-4-hexylthiophen-2-yl)benzo[1,2-b:4,5-b']dithiophene (BDT) and di-borylated-BDT were prepared according to published procedures.[63] Both $BDT(DPP)_2$ and p-BDT-DPP were synthesized using palladium-catalysed Suzuki coupling reactions. The detailed experimental procedure and full characterization of all new materials is presented in the Supplementary Information.

5.2. Film preparation

Glass substrates with dimensions of 2.5 cm × 2.5 cm × 0.1 cm were cleaned by sonicating sequentially in acetone, isopropanol and chloroform. Before thin film casting, the substrates were dried with a strong flow of nitrogen and then subjected to UV/ozone treatment for 30 min. Solutions of $BDT(DPP)_2$ or p-BDT-DPP were prepared by dissolving the samples into chloroform with a concentration of 1 mg/100 µL, respectively. To prepare blend films for sensitized experiments, solutions of $BDT(DPP)_2$ or p-BDT-DPP in chloroform mixed with palladium octaethyl porphyrin (PdOEP), were prepared by dissolving the compounds with mass ratio of 60:40 (sensitizer:organic dye). Solutions were then set to stir overnight in the dark under ambient conditions. Finally, thin films were cast onto clean glass substrates via spin coating at 1000 rpm/s and spun for 1 min.

5.3. Steady state spectroscopy

Absorption spectra were recorded for $BDT(DPP)_2$, p-BDT-DPP and DPP samples using a Varian Cary 50 UV–vis spectrophotometer. Fluorescence spectra were recorded on a Varian Eclipse spectrofluorimeter using excitation wavelengths of 630, 730 and 550 nm for $BDT(DPP)_2$, p-BDT-DPP and DPP, respectively.

Photoluminescence (PL) spectra in the near-IR region were recorded with a spectrometer (Horiba Jobin Yvon iHR320) and an amplified InGaAs photo-detector (Electro-Optical System). The excitation source was a supercontinuum laser (NKT Photonics, SuperK Extreme) for excitation wavelengths tunable across the 450-750 nm region. The excitation beam was mechanically chopped and the detector output was fed into a lock-in amplifier synchronized to the chopper frequency. A 750 nm high pass filter was used to remove the second order of the excitation and fluorescence. PL experiments at cryogenic temperatures were carried out in a liquid nitrogen cryostat (Oxford Instruments, Optistat DN).

Time-correlated single photon counting (TCSPC) in the near-IR region (800 nm) was performed using the supercontinuum laser described above as the excitation source at a pulse repetition rate of 7.8 MHz, and a single photon avalanche diode (EG&G Optoelectronics, SPCM) coupled to the NIR spectrometer described above.

5.4 Cyclic voltammetry

Cyclic voltammetry (CV) experiments were performed at a sweep rate of 100 mVs^{-1} (Solartron). The supporting electrolyte was 0.10 M tetrabutylammonium hexafluorophosphate (Bu_4NPF_6) in DCM. The solutions were deoxygenated by sparging with argon prior to each scan and blanketed with argon during the scans. The glassy carbon working electrode was prepared by polishing with 5mm alumina, washed and dried. The

ferrocene/ferrocenium redox couple was used as a standard. The HOMO and LUMO energy levels were calculated from the onset of the oxidation and reduction potential of the compounds as: E (HOMO)= -($E_{1/2,\ ox\ vs\ Fc+/Fc}$+5.1) eV and E(LUMO)= -($E_{1/2,\ red\ vs\ Fc+/Fc}$+5.1) eV.

5.5. Sub-nanosecond Transient absorption spectroscopy

A mode-locked Ti:sapphire oscillator (Coherent, Mira Seed) seeded a Ti:sapphire regenerative amplifier system (Coherent, RegA 9050) to produce pulses of about 50 fs duration at a repetition rate of 92 kHz and a wavelength centered at 800 nm. A portion of the light was used to generate the 400 nm pump beam using a BBO (barium borate) crystal, and the 630 and 730 nm pump beams were generated with an optical parametric amplifier (OPA9450, Coherent). The pump beam was mechanically chopped at ~3.5 kHz, and the arrival time of the pump pulses relative to the probe was manipulated using a variable optical delay line (Newport, UTS150PP with ESP 300 controller). The broadband probe was derived from the residual 800 nm beam focused onto a 3 mm sapphire substrate (Crystal Systems) for measurements in the visible region (450–800 nm) and a 5 mm undoped YAG substrate (Crystal Systems) for the infrared region (800–1400 nm). After passing through the sample, the probe beam was analyzed with a CMOS detector (Ultrafast Systems) at 7077 spectra/s, and the excess 800 nm laser fundamental was blocked using low- and high-pass filters for the visible and IR regions, respectively. The relative orientation of the pump and probe polarization was 54.7° and all spectra were corrected for the chirp of the supercontinuum probe. Nitrogen was blown over films for all measurements.[64]

5.6. Nanosecond visible transient absorption measurements

Nanosecond visible transient absorption spectroscopy (ns-TA) was employed to monitor the triplet excited state lifetime of BDT(DPP)$_2$. The measurements were conducted by a home-built transient absorption spectrometer with a N_2 laser (LTB Lasertechnik Berlin GmbH, MNL 202-C) pumped dye laser (LTB Lasertechnik Berlin GmbH, ATM200, 700 ps pulse duration) as an excitation source. Transient absorption signal was probed by a Xe lamp (Photon Technology International) light through two monochromators (Acton, Princeton Instruments), and detected by a Si based nanosecond detection system (Unisoku Co., Ltd., TSP-2000SN, time resolution: 1.2 ns (FWHM), monitoring wavelengths: 400~1,100 nm) with a fast oscilloscope (Tektronix, TDS 3052C, Digital Phosphor Oscilloscope 500 MHz 5 GS/s).[65] Transient data were collected with 400 nm excitation with a repetition rate of 2 Hz at 22 °C. The pulse excitation intensity was adjusted to 30 μJ/cm^2.

Nanosecond near infrared transient absorption spectroscopy (ns-TA) was employed to monitor the triplet excited state lifetime of p-BDT-DPP. The measurements were conducted by a home-built transient absorption spectrometer with a Nd:YAG laser (EKSPLA, NT340 series, 5 ns pulse duration) as an excitation source. Transient absorption signal was probed by a Xe lamp light, and detected by a InGaAs based nanosecond detection system (Thorlabs, DET20C/M, time rise: 25 ns, monitoring wavelengths: 800~1700 nm) with a fast oscilloscope (Tektronix, TDS 520, Two channel digitizing Oscilloscope 500 MHz 500 MS/s). Transient data were collected with 550 nm excitation with a repetition rate of 10 Hz. The pulse excitation intensity was adjusted to 30 μJ/cm^2.

5.7. Computational details

All of our calculations were performed with the Gaussian09 program Rev. E.01.[66] The geometry optimization of the ground state was carried out using dispersion-corrected density functional theory (DFT) at the TPSS-D3(BJ)[67-69] /6-311G(d)[70] level of theory and the environmental effects have been taken into account through the polarizable continuum model (IEFPCM)[71] using ethanol as a solvent. In order to reduce computational costs, we have replaced the long side chains in the compound by methyl groups, as the length of the alkyl chains has no significant impact on the optical properties.[72] Vertical excitation energies and partial atomic charges of the electronically states were calculated via time dependent density functional theory within the Tamm-Dancoff Approximation (TDA-DFT)[39] using the CAM-B3LYP[40] range-separated hybrid functional approximation and the 6-311G**[70] atomic-orbital basis set and IEFPCM based on the optimized geometry. A range-separated density functional approximation was chosen to ensure that potential charge-transfer (CT) states could also be appropriately treated. Moreover, it has been shown that this method is one of the most accurate hybrid functional approximations with an expected accuracy of 0.18 eV for medium-sized and large chromophores.[48] The pairs of hole and electron natural-transition-orbitals (NTOs)[73] for the S_1 and T_1 states were calculated to assess the CT and locally excited (LE) contribution of each excited state. DFT and TD-DFT calculation of partial atomic charge (PAC) were conducted using the Merz-Kollman (MK)[74] scheme. The method to define the CT distance (d_{CT}), the transferred charge (q_{CT}), the dipole (μ_{CT}) and H index based on the partial atomic charges is discussed in detail in the supplementary information, and is similar to the procedure described by Jacquemin et al.[44]

Supporting Information

Supporting Information is available from the Wiley Online Library or from the author.

Acknowledgements

This work was made possible by support from the Australian Renewable Energy Agency which funds the project grants within the Australian Centre for Advanced Photovoltaics. Responsibility for the views, information or advice expressed herein is not accepted by the Australian Government. LG was supported by a DECRA Fellowship until April 2017 (DE140100550) and would also like to acknowledge generous allocations of computational resources from the University of Melbourne and the National Computational Infrastructure Facility within the National Computational Merit Allocation Scheme. This work was partly supported by the JST PRESTO program (Photoenergy Conversion Systems and Materials for the Next Generation Solar Cells), Japan.

Reference

[1] M. B. Smith, J. Michl, *Chem. Rev.* **2010**, 110, 6891.
[2] W.-L. Chan, M. Ligges, X. Zhu, *Nat. Chem.* **2012**, 4, 840.
[3] J. C. Johnson, A. J. Nozik, J. Michl, *Acc. Chem. Res.* **2013**, 46, 1290.
[4] S. Singh, W. Jones, W. Siebrand, B. Stoicheff, W. Schneider, *J. Chem. Phys.* **1965**, 42, 330.
[5] W. Shockley, H. J. Queisser, *J. Appl. Phys.* **1961**, 32, 510.
[6] M. J. Tayebjee, D. R. McCamey, T. W. Schmidt, *J. Phys. Chem. Lett.* **2015**, 6, 2367.
[7] R. D. Pensack, E. E. Ostroumov, A. J. Tilley, S. Mazza, C. Grieco, K. J. Thorley, J. B. Asbury, D. S. Seferos, J. E. Anthony, G. D. Scholes, *J. Phys. Chem. Lett.* **2016**, 7, 2370.
[8] J. J. Burdett, C. J. Bardeen, *J. Am. Chem. Soc.* **2012**, 134, 8597.
[9] N. Geacintov, M. Pope, F. Vogel, *Phys. Rev. Lett.* **1969**, 22, 593.
[10] C. Zenz, G. Cerullo, G. Lanzani, W. Graupner, F. Meghdadi, G. Leising, S. De Silvestri, *Phys. Rev. B* **1999**, 59, 14336.
[11] A. Akdag, A. Wahab, P. Beran, L. Rulisek, P. I. Dron, J. Ludvik, J. Michl, *J. Org. Chem.* **2014**, 80, 80.
[12] C. C. Gradinaru, J. T. Kennis, E. Papagiannakis, I. H. van Stokkum, R. J. Cogdell, G. R. Fleming, R. A. Niederman, R. van Grondelle, *Proc. Natl. Acad. Sci. U.S.A.* **2001**, 98, 2364.
[13] C. Wang, M. J. Tauber, *J. Am. Chem. Soc.* **2010**, 132, 13988.
[14] U. Huynh, T. Basel, T. Xu, L. Lu, T. Zheng, L. Yu, V. Vardeny, presented at Proc. SPIE, Physical Chemistry of Nanomaterials and Interfaces XIII **2014**, 9165, 91650Z.
[15] P. Tavan, K. Schulten, *Phys. Rev. B* **1987**, 36, 4337.
[16] J. C. Johnson, A. Akdag, M. Zamadar, X. Chen, A. F. Schwerin, I. Paci, M. B. Smith, Z. k. Havlas, J. R. Miller, M. A. Ratner, *J. Phys. Chem. B* **2013**, 117, 4680.
[17] A. M. Müller, Y. S. Avlasevich, K. Müllen, C. J. Bardeen, *Chem. Phys. Lett.* **2006**, 421, 518.
[18] J. Xia, S. N. Sanders, W. Cheng, J. Z. Low, J. Liu, L. M. Campos, T. Sun, *Adv. Mater.* **2017**, 29.

[19] D. N. Congreve, J. Lee, N. J. Thompson, E. Hontz, S. R. Yost, P. D. Reusswig, M. E. Bahlke, S. Reineke, T. Van Voorhis, M. A. Baldo, *Science* **2013**, 340, 334.

[20] I. Paci, J. C. Johnson, X. Chen, G. Rana, D. Popović, D. E. David, A. J. Nozik, M. A. Ratner, J. Michl, *J. Am. Chem. Soc.* **2006**, 128, 16546.

[21] S. T. Roberts, R. E. McAnally, J. N. Mastron, D. H. Webber, M. T. Whited, R. L. Brutchey, M. E. Thompson, S. E. Bradforth, *J. Am. Chem. Soc.* **2012**, 134, 6388.

[22] E. Busby, J. Xia, Q. Wu, J. Z. Low, R. Song, J. R. Miller, X. Zhu, L. M. Campos, M. Y. Sfeir, *Nat. Mater.* **2015**, 14, 426.

[23] N. A. Pace, W. Zhang, D. H. Arias, I. McCulloch, G. Rumbles, J. C. Johnson, *Phys. Chem. Lett.* **2017**, 8, 6086.

[24] B. Kraabel, D. Hulin, C. Aslangul, C. Lapersonne-Meyer, M. Schott, *Chem. Phys.* **1998**, 227, 83.

[25] A. J. Musser, M. Al-Hashimi, M. Maiuri, D. Brida, M. Heeney, G. Cerullo, R. H. Friend, J. Clark, *J. Am. Chem. Soc.* **2013**, 135, 12747.

[26] Y. Kasai, Y. Tamai, H. Ohkita, H. Benten, S. Ito, *J. Am. Chem. Soc* **2015**, 137, 15980.

[27] A. B. Pun, S. N. Sanders, E. Kumarasamy, M. Y. Sfeir, D. N. Congreve, L. M. Campos, *Adv. Mater.* **2017**, 29, 1701416.

[28] S. N. Sanders, E. Kumarasamy, A. B. Pun, M. L. Steigerwald, M. Y. Sfeir, L. M. Campos, *Chem* **2016**, 1, 505.

[29] S. Sharifzadeh, P. Darancet, L. Kronik, J. B. Neaton, *J. Phys. Chem. Lett.* **2013**, 4, 2197.

[30] E. A. Margulies, C. E. Miller, Y. Wu, L. Ma, G. C. Schatz, R. M. Young, M. R. Wasielewski, *Nat. Chem.* **2016**, 8, 1120.

[31] D. Beljonne, H. Yamagata, J. Brédas, F. Spano, Y. Olivier, *Phys. Rev. Lett.* **2013**, 110, 226402.

[32] W.-L. Chan, M. Ligges, A. Jailaubekov, L. Kaake, L. Miaja-Avila, X.-Y. Zhu, *Science* **2011**, 334, 1541.

[33] M. B. Smith, J. Michl, *Annu. Rev. Phys. Chem.* **2013**, 64, 361.

[34] O. Varnavski, N. Abeyasinghe, J. Aragó, J. J. Serrano-Pérez, E. Ortí, J. T. Lopez Navarrete, K. Takimiya, D. Casanova, J. Casado, T. Goodson III, *J. Phys. Chem. Lett.* **2015**, 6, 1375.

[35] P. E. Hartnett, E. A. Margulies, C. M. Mauck, S. A. Miller, Y. Wu, Y.-L. Wu, T. J. Marks, M. R. Wasielewski, *J. Phys. Chem. B* **2016**, 120, 1357.

[36] C. M. Mauck, P. E. Hartnett, E. A. Margulies, L. Ma, C. E. Miller, G. C. Schatz, T. J. Marks, M. R. Wasielewski, *J. Am. Chem. Soc* **2016**, 138, 11749.

[37] C. M. Mauck, P. E. Hartnett, Y.-L. Wu, C. E. Miller, T. J. Marks, M. R. Wasielewski, *Chem. Mater.* **2017**, 29, 6810.

[38] T. Mukhopadhyay, A. J. Musser, B. Puttaraju, J. Dhar, R. H. Friend, S. Patil, *J. Phys. Chem. Lett.* **2017**, 8, 984.

[39] S. Hirata, M. Head-Gordon, *Chem. Phys. Lett.* **1999**, 314, 291.

[40] T. Yanai, D. P. Tew, N. C. Handy, *Chem. Phys. Lett.* **2004**, 393, 51.

[41] H. Yamagata, J. Norton, E. Hontz, Y. Olivier, D. Beljonne, J.-L. Brédas, R. Silbey, F. Spano, *J. Chem. Phys.* **2011**, 134, 204703.

[42] E. Busby, J. Xia, J. Z. Low, Q. Wu, J. Hoy, L. M. Campos, M. Y. Sfeir, *J. Phys. Chem. B* **2015**, 119, 7644.

[43] N. Monahan, X.-Y. Zhu, *Annu. Rev. Phys. Chem.* **2015**, 66, 601.

[44] D. Jacquemin, T. Le Bahers, C. Adamo, I. Ciofini, *Phys. Chem. Chem. Phys.* **2012**, 14, 5383.

[45] A. D. Becke, *J. Chem. Phys.* **1993**, 98, 5648.

[46] P. Stephens, F. Devlin, C. Chabalowski, M. J. Frisch, *J. Phys. Chem.* **1994**, 98, 11623.

[47] A. Dreuw, J. L. Weisman, M. Head-Gordon, *J. Chem. Phys.* **2003**, 119, 2943.

[48] L. Goerigk, S. Grimme, *J. Chem. Phys.* **2010**, 132, 184103.

[49] R. S. Szabadai, J. Roth-Barton, K. P. Ghiggino, J. M. White, D. J. Wilson, *Aust. J. Chem.* **2014**, 67, 1330.

[50] Q. Tao, L. Duan, W. Xiong, G. Huang, P. Wang, H. Tan, Y. Wang, R. Yang, W. Zhu, *Dyes and Pigments* **2016**, 133, 153.
[51] A. Pickett, A. Mohapatra, A. Laudari, S. Khanra, T. Ram, S. Patil, S. Guha, *Org. Electron.* **2017**, 45, 115.
[52] T. J. Fauvell, T. Zheng, N. E. Jackson, M. A. Ratner, L. Yu, L. X. Chen, *Chem. Mater.* **2016**, 28, 2814.
[53] F. Bencheikh, D. Duché, C. M. Ruiz, J.-J. Simon, L. Escoubas, *J. Phys. Chem.* **2015**, 119, 24643.
[54] K. Goushi, R. Kwong, J. J. Brown, H. Sasabe, C. Adachi, *J. Appl. Phys.* **2004**, 95, 7798.
[55] S. Reineke, M. A. Baldo, *Sci. Rep.* **2014**, 4, 3797.
[56] A. Völcker, H.-J. Adick, R. Schmidt, H.-D. Brauer, *Chem. Phys. Lett.* **1989**, 159, 103.
[57] N. J. Turro, J. C. Scaiano and V. Ramamurthy, Modern Molecular Photochemistry of Organic Molecules, University Science Books, Sausalito, CA, 2010, ISBN-13: 978-1891389252
[58] S. Khan, S. Mazumdar, *J. Phys. Chem Lett.* **2017**, 8, 5943.
[59] S. N. Sanders, E. Kumarasamy, A. B. Pun, M. T. Trinh, B. Choi, J. Xia, E. J. Taffet, J. Z. Low, J. R. Miller, X. Roy, *J. Am. Chem. Soc* **2015**, 137, 8965.
[60] S. Lukman, K. Chen, J. M. Hodgkiss, D. H. Turban, N. D. Hine, S. Dong, J. Wu, N. C. Greenham, A. J. Musser, *Nat. Commun.* **2016**, 7, 13622.
[61] J. Zirzlmeier, D. Lehnherr, P. B. Coto, E. T. Chernick, R. Casillas, B. S. Basel, M. Thoss, R. R. Tykwinski, D. M. Guldi, *Proc. Natl. Acad. Sci. U.S.A.* **2015**, 201422436.
[62] I. Carmichael, G. L. Hug, *J. Phys. Chem. Ref. Data* **1986**, 15, 1.
[63] P. B. Geraghty, C. Lee, J. Subbiah, W. W. Wong, J. L. Banal, M. A. Jameel, T. A. Smith, D. J. Jones, *Beilstein J. Org. Chem.* **2016**, 12, 2298.
[64] K. N. Schwarz, P. B. Geraghty, D. J. Jones, T. A. Smith, K. P. Ghiggino, *J. Phys. Chem. C* **2016**, 120, 24002.
[65] S. Makuta, M. Liu, M. Endo, H. Nishimura, A. Wakamiya, Y. Tachibana, *Chem. Commun.* **2016**, 52, 673.
[66] M. J. Frisch, G. W. Trucks, H. B. Schlegel, G. E. Scuseria, M. A. Robb, J. R. Cheeseman, G. Scalmani, V. Barone, G. A. Petersson, H. Nakatsuji, X. Li, M. Caricato, A. V. Marenich, J. Bloino, B. G. Janesko, R. Gomperts, B. Mennucci, H. P. Hratchian, J. V. Ortiz, A. F. Izmaylov, J. L. Sonnenberg, Williams, F. Ding, F. Lipparini, F. Egidi, J. Goings, B. Peng, A. Petrone, T. Henderson, D. Ranasinghe, V. G. Zakrzewski, J. Gao, N. Rega, G. Zheng, W. Liang, M. Hada, M. Ehara, K. Toyota, R. Fukuda, J. Hasegawa, M. Ishida, T. Nakajima, Y. Honda, O. Kitao, H. Nakai, T. Vreven, K. Throssell, J. A. Montgomery Jr., J. E. Peralta, F. Ogliaro, M. J. Bearpark, J. J. Heyd, E. N. Brothers, K. N. Kudin, V. N. Staroverov, T. A. Keith, R. Kobayashi, J. Normand, K. Raghavachari, A. P. Rendell, J. C. Burant, S. S. Iyengar, J. Tomasi, M. Cossi, J. M. Millam, M. Klene, C. Adamo, R. Cammi, J. W. Ochterski, R. L. Martin, K. Morokuma, O. Farkas, J. B. Foresman, D. J. Fox, Gaussian, Inc., Wallingford CT, 2016, Gaussian 16 Rev. E.01.
[67] S. Grimme, J. Antony, S. Ehrlich, H. Krieg, *J. Chem. Phys.* **2010**, 132, 154104.
[68] S. Grimme, S. Ehrlich, L. Goerigk, *J. Comput. Chem.* **2011**, 32, 1456.
[69] J. Tao, J. P. Perdew, V. N. Staroverov, G. E. Scuseria, *Phys. Rev. Lett.* **2003**, 91, 146401.
[70] R. Krishnan, J. S. Binkley, R. Seeger, J. A. Pople, *J. Chem. Phys.* **1980**, 72, 650.
[71] E. Cances, B. Mennucci, J. Tomasi, *J. Chem. Phys.* **1997**, 107, 3032.
[72] A. D. Chien, A. R. Molina, N. Abeyasinghe, O. P. Varnavski, T. Goodson III, P. M. Zimmerman, *J. Phys. Chem. C* **2015**, 119, 28258.
[73] R. L. Martin, *J. Chem. Phys.* **2003**, 118, 4775.
[74] U. C. Singh, P. A. Kollman, *J. Comput. Chem.* **1984**, 5, 129.

Designing new compounds based on conjugating strong donor and acceptor building blocks provides a pathway for the generation of new materials suitable for optoelectronic devices. An organic molecule ($BDT(DPP)_2$) and polymer (p-BDT-DPP) based on a donor-acceptor framework comprising benzodithiophene (BDT) as electron rich and bisthiophene-2,5-Dihydropyrrolo[3,4-c]pyrrole-1,4-dione (DPP) as electron deficient were designed, synthesized and investigated for singlet fission.

Keywords: Singlet fission, photophysics, organic photovoltaics, intramolecular singlet fission

Saghar Masoomi-Godarzi[ab], Maning Liu[c], Yasuhiro Tachibana[c], Lars Goerigk[b], Kenneth P. Ghiggino[b], Trevor A. Smith[b] and David J. Jones[ab]*

Solution-processable, solid state donor-acceptor materials for singlet fission